BIOCHEMISTRY
including biophysical chemistry & molecular biology

ARTICLE

pubs.acs.org/biochemistry

Metal Binding Motif in the Active Site of the HDV Ribozyme Binds Divalent and Monovalent Ions

Narayanan Veeraraghavan,[†] Abir Ganguly,[‡] Jui-Hui Chen,[§,∥] Philip C. Bevilacqua,[*,†,‡] Sharon Hammes-Schiffer,[*,‡] and Barbara L. Golden[*,§]

[†]Huck Institutes of Life Sciences and [‡]Department of Chemistry, 104 Chemistry Building, The Pennsylvania State University, University Park, Pennsylvania 16802, United States

[§]Department of Biochemistry, Purdue University, 175 South University Street, West Lafayette, Indiana 47907, United States

Supporting Information

ABSTRACT: The hepatitis delta virus (HDV) ribozyme uses both metal ion and nucleobase catalysis in its cleavage mechanism. A reverse G·U wobble was observed in a recent crystal structure of the precleaved state. This unusual base pair positions a Mg^{2+} ion to participate in catalysis. Herein, we used molecular dynamics (MD) and X-ray crystallography to characterize the conformation and metal binding characteristics of this base pair in product and precleaved forms. Beginning with a crystal structure of the product form, we observed formation of the reverse G·U wobble during MD trajectories. We also demonstrated that this base pair is compatible with the diffraction data for the product-bound state. During MD trajectories of the product form, Na^+ ions interacted with the reverse G·U wobble in the RNA active site, and a Mg^{2+} ion, introduced in certain trajectories, remained bound at this site. Beginning with a crystal structure of the precleaved form, the reverse G·U wobble with bound Mg^{2+} remained intact during MD simulations. When we removed Mg^{2+} from the starting precleaved structure, Na^+ ions interacted with the reverse G·U wobble. In support of the computational results, we observed competition between Na^+ and Mg^{2+} in the precleaved ribozyme crystallographically. Nonlinear Poisson−Boltzmann calculations revealed a negatively charged patch near the reverse G·U wobble. This anionic pocket likely serves to bind metal ions and to help shift the pK_a of the catalytic nucleobase, C75. Thus, the reverse G·U wobble motif serves to organize two catalytic elements, a metal ion and catalytic nucleobase, within the active site of the HDV ribozyme.

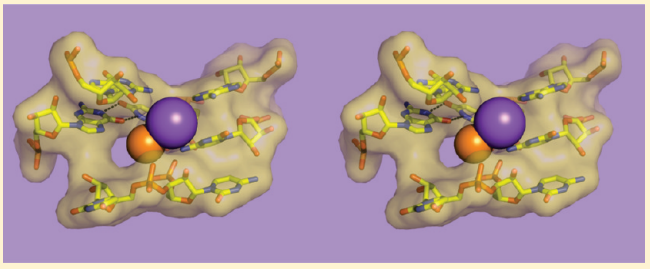

RNA is involved in many aspects of biology, where it serves both informational and functional roles.[1−3] Indeed, RNA can act as a riboswitch, binding small molecules and regulating gene expression,[4,5] and as an enzyme, cleaving phosphodiester bonds during catalysis and driving peptide bond formation on the ribosome.[6] These functions require the RNA to attain a precise three-dimensional structure[7−12] and utilize key catalytic strategies, including general acid−base and metal ion catalysis.[13−16]

A challenge in studying RNA is determining functionally relevant structures at high resolution.[17−22] Over the course of the last 15 years, X-ray crystallography has revolutionized our understanding of RNA structure and function.[23] Crystal structures, however, provide only a snapshot of a molecule, often trapped in a catalytically incompetent state. Furthermore, crystals of RNAs often diffract X-rays to only moderate resolution (2.8 Å or worse), and key catalytic regions within these structures can be disordered.[17−22] As a result, fitting structural models to electron density data can be ambiguous, which can lead to uncertainties in the RNA structure. Even high-resolution crystal structures often have local regions of disorder, and highly ordered regions can change in conformation during the course of a reaction. Theoretical approaches such as molecular dynamics (MD)[24−28] have the potential to both decrease ambiguities in the available RNA crystal structures and provide insight into motions inherent to RNA molecules.

The structure and function of small ribozymes are of growing interest.[6,29] The hepatitis delta virus (HDV) ribozyme occurs as two closely related ∼85 nt double-pseudoknotted genomic and antigenomic versions (Figure 1A) that function to linearize the RNA concatemers that form during replication of the genome.[30−32] A closely related, highly reactive version of this ribozyme also occurs in the human genome in an intron of the *CPEB3* gene.[33,34] Moreover, HDV and HDV-like ribozymes are widespread, occurring in plants, fish, and insects,[35] making their chemical mechanisms of heightened interest.

The HDV ribozyme self-cleaves using a combination of metal ion and general acid−base catalysis, in which a cytosine nucleobase, C75, acts as a general acid and a divalent metal ion acts as a

Received: January 5, 2011
Revised: February 24, 2011
Published: February 24, 2011

dx.doi.org/10.1021/bi2000164 | *Biochemistry* 2011, 50, 2672–2682

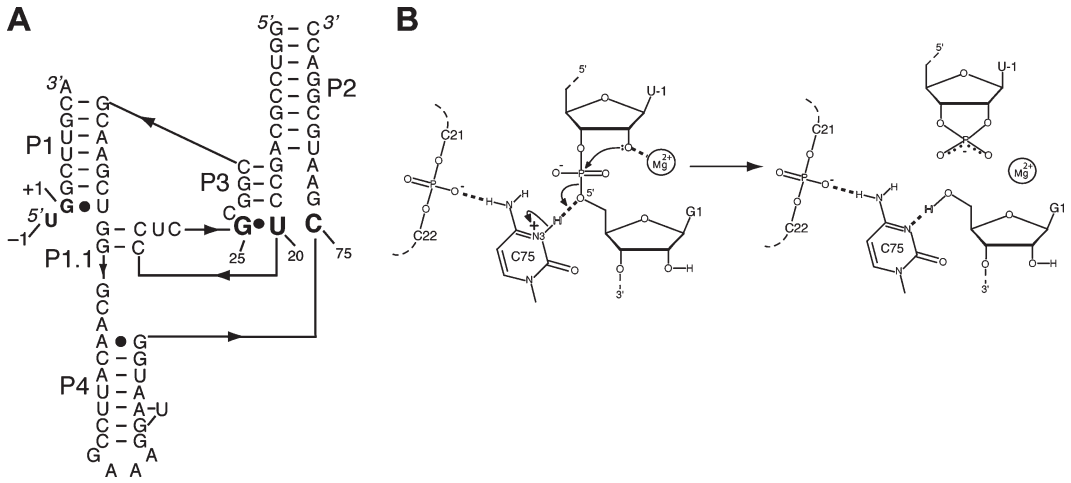

Figure 1. Structure and proposed mechanism of the HDV ribozyme. (A) Secondary structure of the precleaved HDV ribozyme used in a recent crystallography study and herein for MD (PDB ID 3NKB). Numbering is based on the genomic HDV ribozyme.[42] This is a two-piece, fast-folding U27Δ variant,[90] in which P4 has been truncated and modified to facilitate crystallography.[42] The reverse G·U wobble and catalytic C75 residue are in large bold font. The cleavage site is between U-1 and G1, and the five pairing regions are noted as P1−P4 and P1.1. The product ribozyme sequence used for MD is similar to the one shown, but it has a further truncated P4, a joining region between P1 and P2, and a single additional nucleotide insertion, U27, and it lacks the −1 nucleotide.[63] (B) Proposed mechanism of HDV ribozyme self-cleavage in which Mg^{2+} serves as a Lewis acid and C75 as a general acid.[37,39,42] The C75 protonation states depicted in the precleaved and product states are used in the MD simulations.

Lewis acid[36−42] (Figure 1B). The pK_a of C75 is shifted toward neutrality in the precleaved but not the product state,[36,37,43−45] and C75 appears to donate a proton in the cleavage reaction.[39,41,46−48] The role of the divalent metal ion in the reaction is less clear; however, a Mg^{2+} ion in position to interact directly with the 2′-hydroxyl nucleophile is clearly resolved in the crystal structure of the inhibited precleaved HDV ribozyme (PDB ID 3NKB).[42] This metal ion is in position to interact with the pro-R_P oxygen of the scissile phosphate, the pro-S_P oxygen of U23, and, through its hydration shell, the Hoogsteen face of G25. This Mg^{2+} ion also appears to interact with the 2′O of U-1, serving as a Lewis acid. The binding of Mg^{2+} ions within the HDV ribozyme active site is, however, not highly specific. A wide range of divalent ions, including all alkaline earth and even certain transition metals, will react with similar or slightly greater activity.[49,50] In addition, under certain reaction conditions, the ribozyme will react in the absence of divalent ions through a channel in which monovalent ions promote the reaction.[38,51]

In the crystal structure of the inhibited precleaved HDV ribozyme, the nucleotide G25 is in the *syn* conformation, forming a rare reverse wobble base pair with U20.[42] Divalent metal ions are often observed to interact with canonical G·U wobble base pairs through their hydration shells.[52−54] In contrast to Watson−Crick base pairs, canonical G·U wobble pairs provide a concentration of negative dipoles in the major groove that attracts cations. When a reverse G·U wobble is formed with a *syn* G base, a negatively charged surface is also formed, but it is found on the more accessible minor groove face of the helix. Thus, reverse wobbles represent a strategy to create minor-groove metal binding motifs that could be used to facilitate tertiary contacts or the binding of catalytic metal ions.

In this study, we combine crystallographic experiments and all-atom MD calculations to characterize the HDV ribozyme's G25·U20 reverse wobble. We observe that this base pair is stable in both precleaved and product forms of the HDV ribozyme. In contrast, the inactive C75U variant of the ribozyme does not support formation of a reverse G25·U20 wobble pair. Our investigations indicate that the reverse wobble base pair contributes to a negatively charged pocket capable of binding either Mg^{2+} or Na^+ ions in both the precleaved and product states of the ribozyme. Moreover, this negatively charged pocket likely contributes to the shifted pK_a of the catalytic nucleobase, C75.[43,44] Identification of this unusual reverse G·U wobble in the active sites of both the precleaved and product structures has key mechanistic implications for both metal ion- and nucleobase-mediated catalytic strategies.

MATERIALS AND METHODS

Molecular Dynamics Simulations. We computed MD trajectories starting with product and precleaved crystal structures, using reactant and product states derived from the genomic HDV ribozyme and consistent with the proposed mechanism (Figure 1B). The product starting structure was obtained from PDB ID 1CX0,[55,56] with P4 truncated by removing residues 48−69 according to standard numbering[32] (B148−B157 in PDB ID 1CX0). C75 was left unprotonated, as pK_a measurements on the product form suggest this is the predominant state under biologically relevant conditions.[43] The precleaved starting structure was derived from PDB ID 3NKB, with the upstream nucleotide and scissile phosphate built as described previously;[42] deoxynucleotides at positions 1 and 2 were converted to ribonucleotides by addition of 2′-hydroxyls with ideal bond lengths and bond angles. For this structure, C75 was protonated at N3, as suggested by pK_a measurements on the precleaved form.[44] The resulting product and precleaved models contained 62 and 73 nucleotides, respectively. Hydrogen atoms were added using Accelrys Discover Studio Visualizer 2.0.

All HDV ribozyme models were solvated with rigid TIP3P waters[57] in a periodically replicated orthorhombic box. Mg^{2+} ions resolved in the crystal structure were included, although divalent metal ions near the U1A binding domain in the product RNA were excluded; in total, 10 and 11 Mg^{2+} ions were included for the product and precleaved states, respectively. Structures

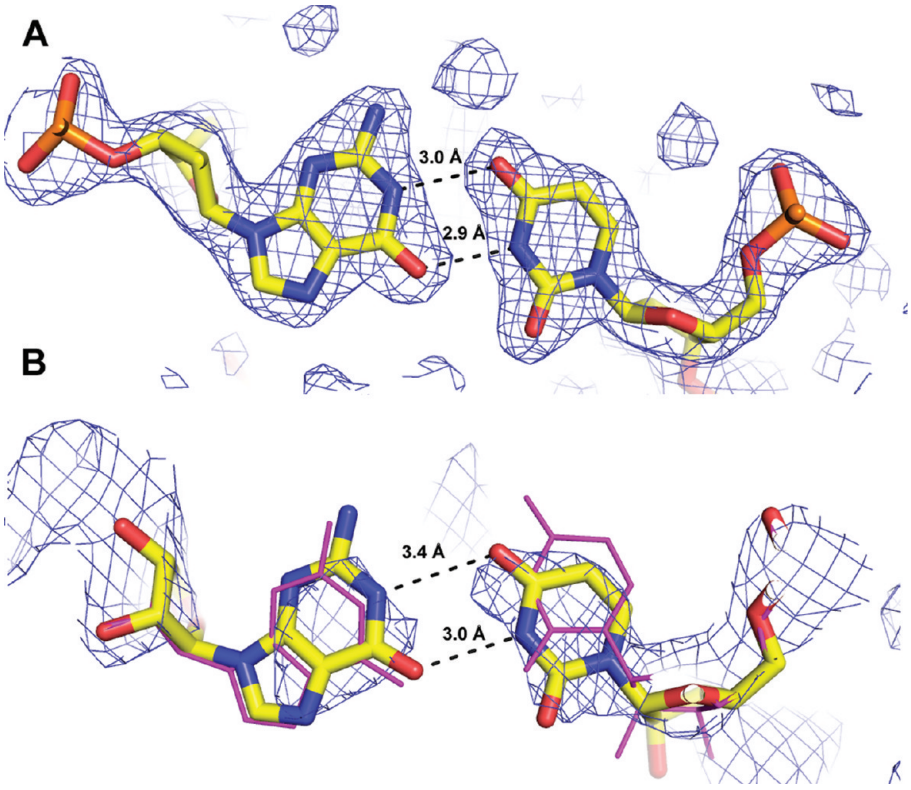

Figure 2. Crystallographic data from the HDV ribozyme product are consistent with formation of a G25·U20 reverse wobble. (A) The G25·U20 reverse wobble from the 1.9 Å crystal structure of the precleaved HDV ribozyme (PDB ID 3NKB).[42] The $2F_o - F_c$ electron density map is contoured at 1σ and drawn within 3 Å of atoms shown. (B) The coordinates of the HDV ribozyme product (PDB ID 1CX0) (magenta lines) do not indicate a G25·U20 reverse wobble pair. This structure was adjusted by a slight rotation of U20 to form a G·U reverse wobble, and the structure was refined as described to generate the model shown in sticks. A 2.3 Å composite simulated annealing omit map contoured at 1σ within 5 Å of the illustrated atoms shows that the crystallographic data are compatible with the G·U reverse wobble geometry.

were neutralized with Na^+ ions, and physiological monovalent ionic strength was added to the solvent to give ~0.15 M NaCl. The force field does not distinguish between Na^+ and K^+ with quantitative accuracy, as discussed previously;[58] thus, the simulations with Na^+ are viewed as qualitatively representative of either monovalent cation.

Calculations were performed with the Desmond MD program[59,60] using the AMBER99 force field,[61,62] as in recent calculations from our laboratories.[63] Partial charges for protonated cytosine were calculated with the RESP method[64,65] using the RED-II program[66] as described previously.[63] Updated charges for protonated cytosine are provided in Supporting Information. Long-range electrostatic interactions were calculated using the smooth particle mesh Ewald method[67] with a cutoff of 12 Å, and SHAKE[68] constraints were applied to bonds involving hydrogen. Following a comprehensive simulated annealing equilibration procedure described in Supporting Information, we collected at least 25 ns of data at 298 K in the canonical ensemble (i.e., constant NVT) for each system. A Nosé-Hoover thermostat[69,70] was used to maintain temperature and pressure, and the time step was 1 fs for all MD trajectories.

Nonlinear Poisson−Boltzmann Analysis. Electrostatic potential calculations were carried out using numerical solutions to the nonlinear Poisson−Boltzmann (NLPB) equation, as described previously.[38,71−73] The calculations were performed with the adaptive Poisson−Boltzmann solver (APBS).[74] Structural coordinates for the precleaved form were obtained from the starting structure for MD, as described above. Structural coordinates for the product form were obtained after extensive equilibration and 20 ns of MD, as described above, in order to allow the reverse G·U wobble to form. Metal ions and water molecules were omitted from NLPB calculations, as per standard protocols.[38,71−73] In addition, C75 was not protonated at N3 in either precleaved or product forms, although C41 was protonated using the updated partial charges provided in the Supporting Information. We chose not to include the catalytic Mg^{2+} ion and not to protonate C75 to enable the assessment of negative potentials that attract these cationic species; we chose to protonate C41 to allow it to maintain its structural triple.[45,56,63,75] Because C41 is ~15 Å from the active site, its electrostatic influence on the protonation of C75 is expected to be small.

For these calculations, the ribozyme was placed in a medium with a dielectric constant of 2 within the solvent-accessible surface-enclosed volume, which was obtained using a probe radius of 1.4 Å. External solvent was treated as a continuum with a dielectric constant of 80, containing a 1:1 electrolyte. A 2.0 Å ion exclusion radius was added to the surface of the RNA to approximate a hydrated sodium ion. A salt concentration of 0.15 M was used in these calculations to mimic physiological conditions.[76,77] Atomic radii and partial charges were defined using the Amber99 parameter set, except for $C41^+$, which was defined as described in the Supporting Information. The calculations were performed with a 97 × 97 × 65 cubic lattice for the product state and a 129 × 65 × 97 cubic lattice for the precleaved

state. The electrostatic potentials were calculated using a sequential focusing procedure.[78] Initial potentials were approximated analytically at lattice points on the boundary of the grid using the Debye−Hückel equation,[79] and solutions were obtained using the sequential focusing method. Three-dimensional structures and electrostatic potentials were rendered using PyMOL.[80]

Crystallographic Refinement of the HDV Ribozyme Postcleavage. Coordinates and data for the product form of the HDV ribozyme were obtained from the Protein Data Bank (PDB ID 1CX0).[55,56] The structure of the ribozyme was adjusted by slightly rotating U20 to allow formation of a reverse G·U wobble pair between G25 and U20. These coordinates were subjected to two rounds of positional and *B*-factor refinement in Phenix[81] to generate a model with reasonable statistics. The original test set was retained in all calculations.

Crystallographic Analysis of the HDV Ribozyme Precleavage. RNA was synthesized and crystallized as described.[42] Prior to data collection, crystals were transferred in a single step to a solution containing 50% 2-methyl-2,4-pentanediol, 50 mM $MgCl_2$, 2 mM spermine, and 50 mM sodium acetate (pH 5.0) for 2−3 h.

Data were collected at GM/CA-CAT of the Advanced Photon Source, beamline 23-ID-D, processed using SCALEPACK20-00,[82] and indexed in space group $C222_1$. An $F_o(K^+) - F_o(Na^+)$ map was calculated using CNS.[83,84] The structure factors $F_o(K^+)$ were obtained from a crystal soaked in potassium-containing cryostabilizing buffer described previously,[42] while the structure factors $F_o(Na^+)$ were obtained from a crystal soaked in sodium-containing cryostabilizing buffer described above (data collection statistics are given in Supporting Information Table S3). Phases were back-calculated from the coordinates of the HDV ribozyme precleavage (PDB ID 3NKB) after removal of the active site Mg^{2+} and solvent molecules.

RESULTS

Overview. We recently solved the structure of the active form of the HDV ribozyme in the presence of C75 and Mg^{2+} at 1.9 Å resolution and pH 5.0.[42] This molecule was trapped precleavage by substituting the 2′-OH of U-1 with a 2′-H (PDB ID 3NKB), thereby removing the nucleophile. In this precleavage structure, a reverse wobble between G25 and U20 was observed, with hydrogen-bonding distances of 2.9−3.0 Å and angles of 172−176° (Figure 2A). This non-Watson−Crick base pair is of interest because it occurs rarely in other RNA structures (J. E. Sokoloski, S. A. Godfrey, and P. C. Bevilacqua, in preparation), the nucleotides involved are conserved in all known HDV and HDV-like ribozymes,[35] and it is located in the active site where it makes key contributions to binding a catalytic metal ion. Moreover, site-directed mutagenesis of these nucleotides has been shown to severely compromise catalytic activity.[85]

We first examined other existing HDV ribozyme crystal structures to determine whether formation of the G25·U20 reverse wobble was a conserved feature. Structural biology of the HDV ribozyme is extensive and includes crystal structures of the product (postcleavage) form (PDB ID 1CX0)[55,56] and a structure of the catalytically inactive C75U mutant bound to an all RNA substrate (PDB ID 1SJ3).[86,87] The G25·U20 reverse wobble is not present in either of these crystal structures. In the product structure (1CX0), G25 is *syn*, but the relative angle between U20 and G25 results in long distances between

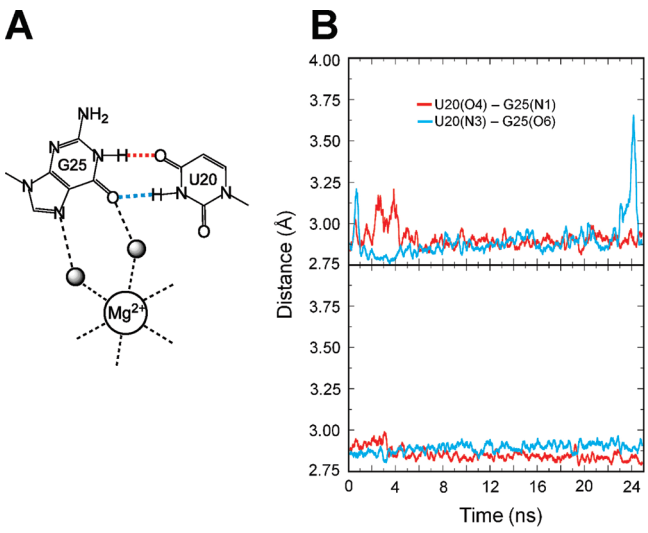

Figure 3. Molecular dynamics simulations of reverse G·U wobble in the product and precleaved forms of HDV ribozyme. (A) Schematic depiction of reverse G·U wobble observed in the crystal structure of the precleaved form.[42] Color coding of the hydrogen bonds is maintained in panel B. (B) Hydrogen-bonding distances in MD trajectory of product C75° state (upper panel). At neutral pH, C75 is deprotonated in the product state.[43] Hydrogen-bonding distances in MD trajectory of precleaved $C75^+$ state (lower panel). In the precleaved state, C75 has a pK_a near neutrality and is largely protonated. Distances plotted are between N and O atoms of each hydrogen bond. See Supporting Information for additional independent MD trajectories.

hydrogen bond donors and acceptors: (U20(O4)−G25(N1) is 5.2 Å and U20(N3)−G25(O6) is 4.2 Å (Figure 2B, magenta structure)[56]). In the C75U mutant structure (1SJ3) G25 is *anti*, precluding reverse wobble pair formation.[86] As the previous crystal structures do not provide evidence for a G25·U20 reverse wobble, we sought herein to explore the stability and metal binding properties of this key structural feature.

MD Analysis of the Reverse G·U Wobble in Product and Precleaved Forms. Previous crystallographic and computational studies on the HDV ribozyme suggested that conformational switching accompanies catalysis.[86,88,89] These studies, however, drew heavily on the structure of the catalytically inactive C75U mutant ribozyme, which has a reorientation of residue 75. To ascertain whether the reverse G25·U20 wobble changes conformation during catalysis, we computed MD trajectories starting with product and precleaved crystal structures, both solved with the wild-type, C75, nucleobase. Given that C75 appears to act as the general acid in cleavage,[37,39,41] we used protonated C75 for the reactant, precleaved state and deprotonated C75 for the product, cleaved state (Figure 1B). Moreover, these protonation states represent the predominant C75 species under biologically relevant buffer conditions on the basis of pK_a measurements[43,44] and are consistent with microscopic reversibility.

As shown in Figure 3B, when beginning with the product form of the ribozyme, during equilibration and throughout the 25 ns trajectory, U20 and G25 form a stable two-hydrogen bond reverse wobble that undergoes only occasional fluctuation of one or the other of the hydrogen bonds. The hydrogen-bonding distances are typically between ∼2.8 and ∼3.1 Å, and the angles U20(O4)−G25(H1)−G25(N1) and U20(N3)−U20(H3)−G25(O6) are ∼160 ± 10°. Notably, these distances and angles are very similar to those observed in the precleaved structure.[42]

Table 1. Metal Ion Residency at the Reverse G·U Wobble Site for Product and Precleaved Forms[a]

structure	trajectory	Mg^{2+} present initially	Mg^{2+} residency (%)	Na^{+} residency (%)
product (C75°)	1	no	0	94
	2	no	0	99
	1	yes	86	12
	2	yes	100	0
precleaved ($C75^{+}$)	1	yes	100	0
	2	yes	100	0
	1	no	0	93
	2	no	0	99

[a] Percentage residency of metal ions at the reverse G·U wobble site for product C75° and precleaved $C75^{+}$ states from MD simulations is presented. Metal ion residency is defined as the percentage of time during the trajectory in which a Mg^{2+} or Na^{+} ion, as appropriate, is located within 5 Å from at least one of the following three atoms: G25(N7), G25(O6), or U20(O2). This distance is consistent with observed second shell ligands.[91] Results are obtained from 25 ns trajectories, with data points taken every 5 ps.

Formation of this reverse wobble was also observed in an independent MD trajectory, with occasional fluctuation of one of the two hydrogen bonds (Supporting Information Figure S2A), and was observed in our previous simulations of the product form.[63] Note that this product crystal structure includes U27, which was omitted in the recent precleaved structure[42] because it is dispensable and U27Δ variants are fast folding.[90] To ascertain the impact of this nucleotide, we propagated an MD trajectory for which U27 was removed from the product crystal structure. We observed formation of the reverse wobble in this case as well (Supporting Information Figure S2C).

We also computed similar trajectories for the C75U precleaved structure. The trajectories on this mutant ribozyme, however, did not result in such hydrogen-bonding interactions between G25 and U20. Instead, over the course of several independent 4.5 ns trajectories, only a one-hydrogen bond interaction involving the N3 of U20 and the Hoogsteen face (either O6 or N7 of G25) formed (data not shown). Sponer, Walter, and colleagues previously conducted MD simulations using the AMBER 99 force field on product and C75U precleaved crystal structures and obtained similar results: a reverse G·U wobble formed in the product structure but not in the C75U mutant structure.[88] Thus, these data suggest that the reverse G·U wobble is compatible with the wild-type base at position 75 but not a U.

To further the analysis, we propagated MD trajectories based on the new precleaved structure, which contains C75 and Mg^{2+}, with the U-1 nucleotide and scissile phosphate.[42] As mentioned above, these MD trajectories were propagated with protonated C75, using the updated atomic charges provided in Supporting Information; in this state, the ribozyme is poised for general acid catalysis. As shown in Figure 3C, the trajectory in the precleaved form indicates that the two hydrogen bonds of the reverse G·U wobble are exceptionally stable, with hydrogen-bonding distances between 2.8 and 3.0 Å and hydrogen-bonding angles of 159−163°, similar to those in the starting structure. Moreover, this stability of the reverse G·U wobble in the precleaved form was reproduced in an independent trajectory (Supporting Information Figure S2B). Overall, the MD data suggest that the wild-type ribozyme does not change conformation at the G25·U20 reverse wobble pair during catalysis and that it is exceptionally stable in the precleaved state.

Crystallographic Analysis of the Reverse G·U Wobble in Product and Precleaved Forms. Lack of hydrogen bonding between U20 and G25 reported in the crystal structure of the product ribozyme could be the result of absence of the scissile phosphate, an artifact of crystal contacts, or because the conformation of these nucleotides may be inadequately restrained by the diffraction data. We therefore examined the crystal structure of the product state, adjusted the positions of G25 and U20 to form the reverse wobble pair, and refined this model using the deposited structure factors (see Materials and Methods). A model with 3.0−3.4 Å hydrogen bonds between the appropriate non-hydrogen atoms in the reverse G·U wobble was attained (Figure 2B), with similar values for R_{free} and R_{work} (Supporting Information Table S6). The composite simulated annealing omit map supports the modified conformation of U20 (Figure 2B). We conclude, therefore, that the original X-ray diffraction data on the product structure are compatible with formation of the reverse G·U wobble, even if they were insufficient to readily define it. Significantly, these results suggest that restraints derived from MD studies could enhance accuracy of crystal structures in regions not adequately restrained by high-quality electron density.

MD Analysis of Metal Ion Binding in Product and Precleaved Forms. In the crystal structure of the precleaved HDV ribozyme, G25 is a second-shell ligand, interacting with the catalytic Mg^{2+} ion through solvent molecules. This ion is absent in the crystal structure of the product HDV ribozyme. We therefore examined MD trajectories of precleaved and product forms to assess whether metal cations can interact with the active site.

For the product structure, Na^{+} ions bound near the reverse wobble during equilibration in two independent MD trajectories. A Na^{+} ion interacted stably within ∼5 Å from the O6 and N7 of G25 and the O2 of U20 (Supporting Information Figure S3 and Table S5) for ∼96% of the time during these trajectories (Table 1). These distances are consistent with a water-mediated interaction between the reverse wobble and the Na^{+} ion.[91] Additionally, sometimes two Na^{+} ions bound to this site (∼7% and ∼40% of the time for the first and second independent trajectories, respectively). Average distances of the Na^{+} ion to the reverse G·U wobble showed a relatively broad distribution, with rmsd values of 1.1−2.7 Å (Supporting Information Figure S3A and Table S5).

Mg^{2+} ions are much less likely to bind to this site in these trajectories because of the relatively low concentration of Mg^{2+} ions in the simulation system. Moreover, the Mg^{2+} ions that were included in the above simulations are expected to exhibit low mobility because they were bound to the ribozyme in the product crystal structure. To probe whether this site is capable of stably binding Mg^{2+}, we therefore propagated two independent trajectories in which we removed two Na^{+} ions from the bulk solvent and inserted a Mg^{2+} ion into the active site so that it was bound to the reverse G·U wobble. We found that the Mg^{2+} remained bound 86% and 100% of the time, with Na^{+} binding 12% and 0% of the time, for the first and second independent trajectories, respectively (Table 1). Average distances of the Mg^{2+} ion to the reverse G·U wobble were again ∼5 Å but displayed a narrower distribution, with rmsd values of only 0.3−1.2 Å (Supporting Information Figure S3B and Table S5). Together, these two sets

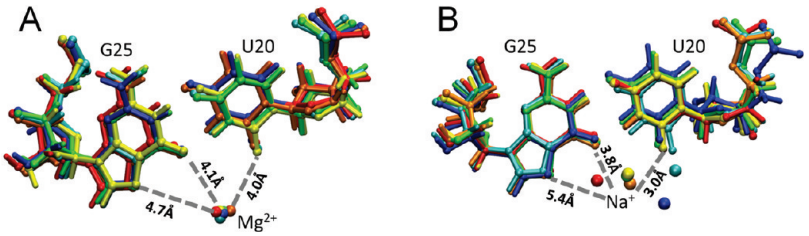

Figure 4. Snapshots of movement of metal ion during MD trajectories of the precleaved C75$^+$ state of the HDV ribozyme. (A) Coordination of Mg^{2+} for a trajectory with Mg^{2+} bound to this site throughout the trajectory. (B) Coordination of Na^+ for a trajectory with the bound Mg^{2+} ion removed from the active site and replaced by two Na^+ ions in the bulk prior to equilibration. The colors show snapshots at various time steps: blue, 0 ns; cyan, 5 ns; green, 10 ns; yellow, 15 ns; orange, 20 ns; red, 25 ns. These results were obtained for a single independent trajectory of each type. (For part B, the 0 ns snapshot is actually a 1.5 ns snapshot to satisfy the criteria for bound Na^+.) The snapshots at these time steps were aligned to minimize the rmsd for the heavy atoms of residues G25 and U20. Average distances between key atoms of the reverse G·U wobble and these metal ions are indicated near the dashed lines. These distances, as well as their standard deviations, are provided as the first trajectory in Supporting Information Table S5. See Supporting Information Figure S3 for the analogous figure for the product C75° state.

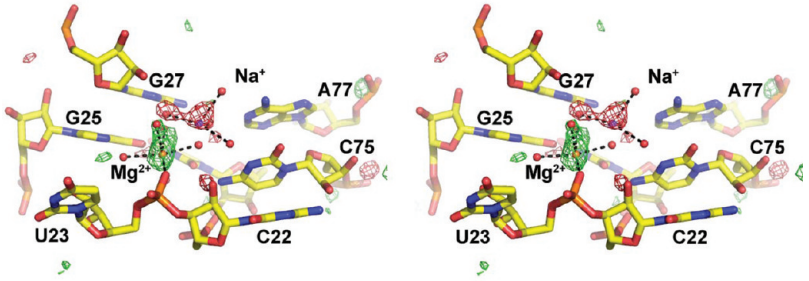

Figure 5. Stereoview of the $F_o(K^+) - F_o(Na^+)$ difference Fourier map of the precleaved HDV ribozyme. Data to 1.9 Å resolution were used to calculate the map. The map is contoured at 3σ (green) and at -3σ (red) within 5 Å of every atom shown. Positive peaks represent atoms that are present at higher occupancy in the absence of Na^+ ion, while negative peaks represent atoms that are present at higher occupancy in the presence of Na^+. Mg^{2+} and Na^+ ions, colored orange and purple, respectively, are observed at competing sites within the HDV ribozyme active site.

of results suggest that either Na^+ or Mg^{2+} could potentially bind to the reverse G·U wobble in the product state. Due to limitations of the MD simulations, however, we are unable to predict the probabilities or strength of such binding.

When trajectories were propagated with the precleaved structure containing the crystallographically observed active site Mg^{2+} ion at the reverse wobble,[42] the Mg^{2+} ion remained bound 100% of the time for both MD trajectories (Table 1), and its distances of ~4.3 Å were relatively static, with rmsd values of 0.2 Å (Figure 4A and Supporting Information Table S5). For comparison, MD trajectories were computed in which this Mg^{2+} ion was removed from the active site and two additional Na^+ ions were placed in the bulk. We observed that Na^+ ions bound to the reverse wobble during the majority of these trajectories. Specifically, at least one Na^+ ion interacted stably with the reverse wobble for ~96% of the time (Table 1). The distribution of distances between the Na^+ ion and the reverse G·U wobble was broader than that observed for the Mg^{2+} ion, with average distances ranging from ~3 to 7 Å and rmsd values of 0.4−1.5 Å (Figure 4B and Supporting Information Table S5).

In summary, both monovalent and divalent ions bound to both product and precleaved forms of the HDV ribozyme in the MD simulations. There appears to be a preference for binding of divalent ions to the precleaved state because residency was 100% and there was essentially no movement of the Mg^{2+} ion as compared to other metal ion/ribozyme state combinations. This observation is qualitatively consistent with experimental data indicating stronger binding of Mg^{2+} than Na^+.[49,50] However, limited sampling in the MD trajectories prevents a quantitative analysis of the relative probabilities and binding strengths.

Crystallographic Analysis of Metal Ion binding in the Precleaved Form. The MD trajectories described in the preceding section exhibited binding of either Na^+ or Mg^{2+} in the HDV ribozyme active site. We wanted to assess the extent to which these calculations are supported by in vitro experimental data. Prior results from our laboratory indicated that increasing the concentration of Na^+ above 200 mM inhibits self-cleavage in the presence of 1 mM Mg^{2+}, consistent with competition between these ions.[50] Moreover, Hill analysis of these data, which was conducted at high ionic strength of 0.3−2 M to separate out folding effects, supported displacement of the Mg^{2+} ion by 1.7 ± 0.2 Na^+ ions. Monovalent ions are known to support cleavage by an alternative reaction mechanism,[50,51] making it possible that Na^+ ions observed herein participate in catalysis by this alternative reaction channel.

We therefore examined whether competition between the Mg^{2+} and Na^+ ions could be observed crystallographically. Two crystals of the HDV ribozyme that varied only in the counterion used in the cryostabilization buffer were compared. An $F_o(K^+) - F_o(Na^+)$ difference Fourier map should contain positive peaks representing features present in K^+ but absent or smaller in the presence of Na^+. Likewise, features present in Na^+ buffers but absent in K^+ will be revealed by negative peaks in the map (Figure 5). We observed that, in the presence of Na^+, the active site Mg^{2+} has reduced occupancy and a Na^+ binding site lies nearby. Simultaneous binding of Mg^{2+} and Na^+ to this site is

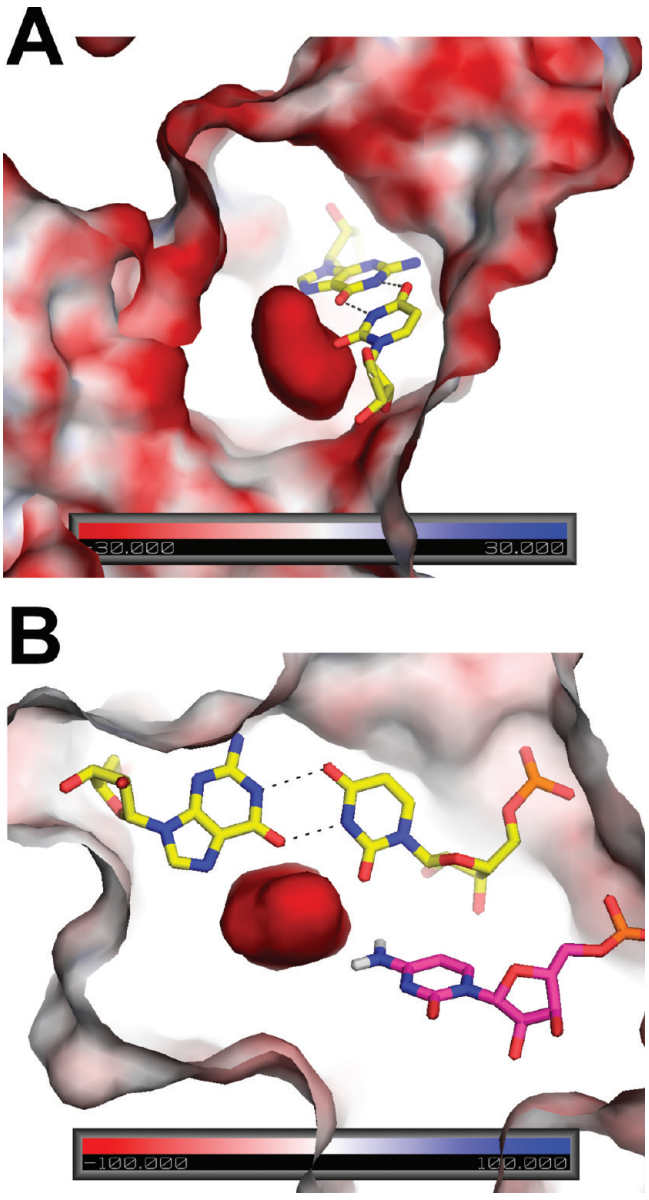

Figure 6. Surface electrostatic potential of precleaved HDV ribozyme. The potential is colored according to the scales provided in the base of each panel. The scale for panel A is −30 to +30 kT/e, while the scale for panel B is −100 to +100 kT/e. Views shown here are near the reverse G·U wobble, which is depicted in yellow sticks with hydrogen bonding in black. (A) Orientation showing large negative potential in the center, which reaches values greater in magnitude than −100 kT/e. Analogous figure for the product state of the HDV ribozyme is provided in Supporting Information Figure S5A. (B) Orientation showing interaction of C75 and reverse G·U wobble with negative potential in the precleaved state. C75 is in magenta with N4 hydrogens shown explicitly. Note that the C75 is oriented toward the highly negatively charged pocket generated near the reverse G·U wobble. The amine of C75 is a second shell ligand to the catalytic Mg^{2+} (not shown here) and is hydrogen bonded to the scissile phosphate. View is rotated counterclockwise by ∼90° from panel A and viewed from the top. Details of phosphates contributing to the potential of the precleaved state are provided in Supporting Information Figure S5B.

precluded sterically as well as electrostatically. The positive peak in the $F_o(K^+) - F_o(Na^+)$ difference Fourier map (Figure 5) cannot be due to binding of K^+ at this position as the metal−ligand distances (2.1−2.4 Å) are smaller than those expected for a K^+ ion (∼2.7 Å). In addition, the octahedral coordination geometry is consistent with this ion being a Mg^{2+}. The larger ionic radius of K^+ presumably prevents binding of this ion in the HDV ribozyme active site. Indeed, displacement of Mg^{2+} by K^+ in the active site of group I introns induces significant rearrangements to accommodate the larger cation.[8,92] Thus, these experimental data support competition of Na^+ and Mg^{2+} for binding to the HDV ribozyme site, consistent with MD and biochemical observations. No additional Na^+ binding sites were observed in the $F_o(K^+) - F_o(Na^+)$ difference Fourier map.

Nonlinear Poisson−Boltzmann Calculations. In an effort to discern a physical basis for cation binding to the reverse G·U wobble, we performed NLPB electrostatic calculations on product and precleaved states (Figures 6 and Supporting Information Figure S5). These calculations provide qualitative insight by identifying negatively charged regions of the ribozyme that can serve as possible Na^+ and Mg^{2+} binding sites. We first performed NLPB calculations on the product state with deprotonated C75 at various time steps along the 25 ns trajectory, during which the reverse G·U wobble is present and a Na^+ ion binds (see above). The results for the snapshot at 20 ns are shown in Supporting Information Figure S5A. A negatively charged binding pocket was observed near the reverse G·U wobble, which persisted throughout the simulation.

Next, we carried out NLPB calculations on the precleaved state in which C75 was left deprotonated and Mg^{2+} ions were removed (see Materials and Methods). The charged pocket observed here was significantly more negative (<−100 kT/e in precleaved versus ∼−40 kT/e in product) (Figure 6). The extremely negative potential appearing in the precleaved active site is due in part to positioning of a constellation of phosphates, including the scissile phosphate, in this region (Supporting Information Figure S5B). The negatively charged character of this site probably accounts for the high occupancy of Mg^{2+} in the active site of the precleaved RNA, both in the crystals and in the MD, and may assist in positioning and protonating C75 for catalysis (Figure 6B).

DISCUSSION

The MD and experimental results suggest that a reverse G·U wobble base pair, in conjunction with a constellation of surrounding phosphates, provides a cation binding site within a structured RNA. The reverse G·U wobble motif is unusual in that, outside of UNCG hairpin loops, it has been observed in only one other large RNA (23S rRNA), based on a systematic study of ribozymes in the PDB (J. E. Sokoloski, S. A. Godfrey, and P. C. Bevilacqua, in preparation). Furthermore, this G and U are universally conserved in HDV and HDV-like ribozymes.[35] We observed herein that the reverse G·U wobble in the HDV ribozyme active site is stably formed in both functionally relevant states of the HDV ribozyme (precleaved and product) but is disrupted in the inactive C75U mutant. This conclusion is derived from analyses of crystal structures and MD simulations. Proper formation of this base pair is critical in that it contributes to both the three-dimensional structure of the active site[42] and a highly negatively charged patch within the HDV ribozyme active site. The resulting cation binding site appears to recruit a catalytic Mg^{2+} ion that participates directly in the cleavage reaction. Moreover, the negatively charged character of this site facilitates binding of monovalent ions and protonation of C75[43,44] and may aid in the accurate positioning of this catalytic nucleobase.

A Motif That Contributes to a Negatively Charged Patch in the Minor Groove. Large ribozymes, including group I introns, group II introns, and RNase P, have active site pockets created by the junctions of multiple helices and "single-stranded" RNAs.[8,10,92−94] These complex active sites bring together clusters of two to three negatively charged phosphate groups from the ribozyme core that serve to bind and orient catalytic metal ions. On the other hand, small ribozymes, such as the hammerhead, hairpin, and HDV ribozymes, are only ∼70 nts in length. Their active sites are usually formed by the juxtaposition of two base-paired helices and typically lack the phosphate clusters observed in large ribozymes. It was therefore anticipated that these ribozymes would function by Mg^{2+}-free mechanisms, and indeed all can react in the absence of Mg^{2+}.[37,95]

The crystal structures of the HDV ribozyme provided the first glimpses of a metal ion within a small ribozyme active site positioned to interact with the scissile phosphate.[42] Consistent with the lack of phosphate clusters in small ribozyme active sites, only a single phosphate from the HDV ribozyme core, that of U23, interacts with the catalytic metal ion. This metal binding site is buttressed by a reverse G·U wobble, a motif compatible with the duplex RNA structures often found in small ribozyme active sites. The negative potential of the metal binding pocket is due, in part, to the O6 and N7 of G25 and the O2 of U20 within the minor groove of the RNA helix. This observation is qualitatively consistent with previous observations that canonical G·U wobble pairs bind Mg^{2+} ions in the major groove of RNA helices.[52,53,96−98] A Watson−Crick A-U base pair cannot substitute for the G25-U20 base pair;[85] however, additional work will be required to determine if the G25A mutation disrupts metal binding, the three-dimensional organization of the active site, folding, or a combination of these factors.

In addition to the G25-U20 reverse wobble, the pro-S_P oxygen of U23 and, in the precleavage state, the pro-R_P oxygen of the scissile phosphate cluster to create a negatively charged region within the HDV ribozyme active site. The negative potential in this pocket reaches values of <−100 kT/e (Figure 6), which contributes to metal binding.[71,72] The value of this potential is similar to that for the metal ion binding core of P4−P6,[71] an ∼160 nt independent folding domain of the *Tetrahymena thermophila* ribozyme.[99] Thus, the HDV ribozyme, although having only approximately half the number of nucleotides, can assume a similar negatively charged binding motif in its core. Given that the P4−P6 motif functions in metal binding,[52] it is reasonable that a similarly negatively charged motif in the HDV ribozyme could also function in metal binding.

Despite these similarities, there are also clear differences in catalytic metal ion requirements for the large ribozymes and HDV ribozymes. The former can use Mg^{2+} and sometimes Mn^{2+} for catalysis, while other ions such as Ca^{2+} are inhibitory.[100] In contrast, the HDV ribozymes operate proficiently with a broad range of divalent and monovalent ions, including all alkaline earth and alkali metals, and several transition metals.[49−51] This loosening of specificity may be the result of fewer inner sphere contacts between the ribozyme and the catalytic metal, as well as the flexibility afforded by the water-mediated interactions between the catalytic metal and G25.

Implications for HDV Ribozyme Catalysis. Crystallographic and MD studies support the presence of a cation binding site near the reverse G25·U20 wobble that is capable of binding either Mg^{2+} or Na^+. This anionic pocket likely binds other divalent and monovalent ions that support catalysis. On the basis of these studies and others, we propose that this site binds a catalytic metal ion capable of participating in catalysis, most likely through a Lewis acid mechanism (Figure 1B).[42] These data are consistent with observed inhibition of the Mg^{2+}-dependent ribozyme reaction by sodium or cobalt hexammine ions.[37,50,101] Na^+ ions presumably are capable of displacing the catalytic Mg^{2+} ion, leading to a reduction in ribozyme activity as the ribozyme shifts to a Mg^{2+}-independent reaction channel. Cobalt hexammine is capable of displacing Mg^{2+} from the HDV ribozyme;[86] however, its ligands are nonlabile, and it cannot serve as a Lewis acid. This ion therefore inhibits the reaction by competing with the catalytic Mg^{2+}.

In the presence of Na^+, the ribozyme is capable of Mg^{2+}-free catalysis.[37,38,75] The overall rate of reaction is ∼3000-fold faster in saturating Mg^{2+} than 1 M NaCl, with ∼125-fold due to Mg^{2+} facilitating folding and ∼25-fold due to Mg^{2+} facilitating chemistry. Thus, high concentrations of Na^+ are reasonably effective in facilitating catalysis, a characteristic also observed in the hammerhead ribozyme,[102,103] although the mechanistic involvement of Na^+ ions is unclear in that system. Several lines of evidence suggest that the HDV ribozyme reaction catalyzed by monovalent ions proceeds through an alternative but related mechanism, described previously as a multichannel mechanism.[50] First, the pH−rate profile for the reaction is inverted under Mg^{2+}-free conditions.[37,41,45] Second, proton inventory experiments, which monitor the number of proton transfers in the rate-limiting step, are 2 in low or no Mg^{2+}, but approach 1 in high Mg^{2+} concentration;[47] moreover, similar results, proton inventories of 1 in 10 mM Mg^{2+}, were reported for the antigenomic ribozyme by the Been laboratory.[46] These data are consistent with a model in which Mg^{2+} binding to the U-1 2′-hydroxyl stabilizes deprotonation of the nucleophile, leaving only a single proton transfer, from $C75H^+$ to the O5′ of G1, in the rate-limiting step. When Na^+ displaces Mg^{2+}, the active site cation is bound in a similar location, but it cannot play the role of a Lewis acid. Indeed, solvent isotope effects under these conditions support deprotonation of the 2′OH of U-1 by a hydroxide ion from solution.[41] Na^+ ions in the HDV ribozyme active site have the potential to contribute to the reaction by other catalytic means, such as stabilizing appropriate active site and substrate geometries and contributing to favorable electrostatics.

Contribution of the Motif to Organization of the Active Site. The negatively charged pocket near the G25·U20 reverse wobble not only binds Mg^{2+} and Na^+ ions but also likely contributes to the catalytic properties of C75. The pK_a of C75 is shifted toward 7 in the precleaved state of the ribozyme; however, the pK_a is similar to that of isolated cytosine in the product form of the ribozyme.[43−45] Given that electrostatics help to drive protonation of the nucleobases in general,[104] the positioning of the phosphates, including the scissile phosphate in the precleaved state, likely helps to drive the pK_a of C75 toward neutrality (Figure 6B and Supporting Information Figure S5B). Moreover, protonation of C75 is coupled anticooperatively with binding of Mg^{2+} ions.[37,44,45] The negative potential of this pocket appears extreme enough to engage both a divalent metal ion and a positively charged base, helping to explain these previous experimental results.

Lastly, this motif may help to position C75 properly for catalysis. According to our calculations of partial charges for protonated cytosine, the H4s on $C75^+$ carry a total net charge of +0.93, while H3 has a charge of just +0.30 (Supporting Information Table S2). These partial charges are consistent with

crystal structures of the HDV ribozyme,[42] where the H4s of $C75^+$, rather than H3, orient toward this patch. This positioning is critical because it leaves the H3 positioned for proton transfer to the O5′ of G1. Previous MD simulations based on an alternative starting structure, in which the C75U crystal structure was mutated back to $C75^+$ and using different partial charges for $C75^+$, resulted in the H3 of C75 being recruited to the negatively charged phosphate of G1 rather than its O5′.[88]

Conclusions. In this paper, we presented evidence that a reverse G·U wobble interaction capable of binding Na^+ and Mg^{2+} ions is present in both precleaved and product states of the HDV ribozyme. This evidence was obtained from analyses of crystallographic data and MD simulations. Moreover, electrostatic potential calculations indicated that formation of the reverse G·U wobble contributes to a highly negatively charged patch within the HDV ribozyme active site, thereby facilitating the binding of metal ions and the positioning of the catalytic protonated C75. The existence of the metal binding reverse G·U wobble in both the precleaved and product states supports the mechanistic hypothesis that the catalytic metal is retained throughout the reaction. Thus, appropriate combinations of experimental data, structural models, and MD simulations have the potential to uncover catalytically relevant interactions from RNA crystal structures.

■ ASSOCIATED CONTENT

Supporting Information. Procedures for MD; protonated cytosine partial charges; additional MD trajectories; metal ion movement during MD; heavy-atom rmsd plots; additional NLPB results; tables of crystallographic data collection statistics; crystallographic Na^+ coordinates for the precleaved ribozyme; and average distances between the reverse G·U wobble and metal ions from MD. This material is available free of charge via the Internet at http://pubs.acs.org.

■ AUTHOR INFORMATION

Corresponding Author

*B.L.G.: telephone, (765) 496-6165; fax, (765) 494-7897; e-mail, barbgolden@purdue.edu. S.H.-S.: telephone, (814) 865-6442; fax, (814) 865-2927; e-mail, shs@chem.psu.edu. P.C.B.: telephone, (814) 863-3812; fax, (814) 865-2927; e-mail, pcb@chem.psu.edu.

Present Addresses

[||] Department of Biochemistry, University of Illinois, 600 S. Mathews Ave., Urbana, IL 61801.

Funding Sources

This project was supported by NIH Grant R01GM095923 (B.L.G. and P.C.B.) and NIH Grant GM56207 (S.H.-S.); instrumentation was funded by the NSF through Grant OCI-0821527, the Purdue University Department of Biochemistry, the Markey Center for Structural Biology, and the Purdue University Center for Cancer Research (B.L.G.).

■ ACKNOWLEDGMENT

We thank Alexander Soudackov for helpful discussions.

■ ABBREVIATIONS

HDV, hepatitis delta virus; MD, molecular dynamics; NLPB, nonlinear Poisson−Boltzmann.

■ REFERENCES

(1) Copley, S. D., Smith, E., and Morowitz, H. J. (2007) The origin of the RNA world: co-evolution of genes and metabolism. *Bioorg. Chem. 35*, 430–443.

(2) Cech, T. R. (2009) Crawling out of the RNA world. *Cell 136*, 599–602.

(3) Turk, R. M., Chumachenko, N. V., and Yarus, M. (2010) Multiple translational products from a five-nucleotide ribozyme. *Proc. Natl. Acad. Sci. U.S.A. 107*, 4585–4589.

(4) Henkin, T. M. (2008) Riboswitch RNAs: using RNA to sense cellular metabolism. *Genes Dev. 22*, 3383–3390.

(5) Roth, A., and Breaker, R. R. (2009) The structural and functional diversity of metabolite-binding riboswitches. *Annu. Rev. Biochem. 78*, 305–334.

(6) Fedor, M. J. (2009) Comparative enzymology and structural biology of RNA self-cleavage. *Annu. Rev. Biophys. 38*, 271–299.

(7) Holbrook, S. R. (2005) RNA structure: the long and the short of it. *Curr. Opin. Struct. Biol. 15*, 302–308.

(8) Golden, B. L., Kim, H., and Chase, E. (2005) Crystal structure of a phage Twort group I ribozyme-product complex. *Nat. Struct. Mol. Biol. 12*, 82–89.

(9) Martick, M., and Scott, W. G. (2006) Tertiary contacts distant from the active site prime a ribozyme for catalysis. *Cell 126*, 309–320.

(10) Toor, N., Keating, K. S., Taylor, S. D., and Pyle, A. M. (2008) Crystal structure of a self-spliced group II intron. *Science 320*, 77–82.

(11) Montange, R. K., and Batey, R. T. (2008) Riboswitches: emerging themes in RNA structure and function. *Annu. Rev. Biophys. 37*, 117–133.

(12) Jinek, M., and Doudna, J. A. (2009) A three-dimensional view of the molecular machinery of RNA interference. *Nature 457*, 405–412.

(13) Narlikar, G. J., and Herschlag, D. (1997) Mechanistic aspects of enzymatic catalysis: lessons from comparison of RNA and protein enzymes. *Annu. Rev. Biochem. 66*, 19–59.

(14) DeRose, V. J. (2003) Metal ion binding to catalytic RNA molecules. *Curr. Opin. Struct. Biol. 13*, 317–324.

(15) Sigel, R. K., and Pyle, A. M. (2007) Alternative roles for metal ions in enzyme catalysis and the implications for ribozyme chemistry. *Chem. Rev. 107*, 97–113.

(16) Bevilacqua, P. C. (2008) Proton transfer in ribozyme catalysis, in *Ribozymes and RNA Catalysis* (Lilley, D. M., and Eckstein, F., Eds.) pp 11−36, Royal Society of Chemistry, Cambridge, U.K.

(17) Cate, J. H., and Doudna, J. A. (2000) Solving large RNA structures by X-ray crystallography. *Methods Enzymol. 317*, 169–180.

(18) Ferre-D'Amare, A. R., and Doudna, J. A. (2001) Methods to crystallize RNA, in *Current Protocols in Nucleic Acid Chemistry*, Chapter 7, Unit 7 6.

(19) Egli, M. (2004) Nucleic acid crystallography: current progress. *Curr. Opin. Chem. Biol. 8*, 580–591.

(20) Golden, B. L. (2007) Preparation and crystallization of RNA. *Methods Mol. Biol. 363*, 239–257.

(21) Yajima, R., Proctor, D. J., Kierzek, R., Kierzek, E., and Bevilacqua, P. C. (2007) A conformationally restricted guanosine analog reveals the catalytic relevance of three structures of an RNA enzyme. *Chem. Biol. 14*, 23–30.

(22) Spitale, R. C., and Wedekind, J. E. (2009) Exploring ribozyme conformational changes with X-ray crystallography. *Methods 49*, 87–100.

(23) Nilsen, T. W. (2007) RNA 1997−2007: a remarkable decade of discovery. *Mol. Cell 28*, 715–720.

(24) Vaiana, A. C., Westhof, E., and Auffinger, P. (2006) A molecular dynamics simulation study of an aminoglycoside/A-site RNA complex: conformational and hydration patterns. *Biochimie 88*, 1061–1073.

(25) Kormos, B. L., Baranger, A. M., and Beveridge, D. L. (2006) Do collective atomic fluctuations account for cooperative effects? Molecular dynamics studies of the U1A-RNA complex. *J. Am. Chem. Soc. 128*, 8992–8993.

(26) McDowell, S. E., Spackova, N., Sponer, J., and Walter, N. G. (2007) Molecular dynamics simulations of RNA: an in silico single molecule approach. *Biopolymers 85*, 169–184.

(27) Lee, T. S., Lopez, C. S., Giambasu, G. M., Martick, M., Scott, W. G., and York, D. M. (2008) Role of Mg(2+) in hammerhead ribozyme catalysis from molecular simulation. *J. Am. Chem. Soc. 130*, 3053–3064.

(28) Lee, T. S., Giambasu, G. M., Sosa, C. P., Martick, M., Scott, W. G., and York, D. M. (2009) Threshold occupancy and specific cation binding modes in the hammerhead ribozyme active site are required for active conformation. *J. Mol. Biol. 388*, 195–206.

(29) Ferre-D'Amare, A. R., and Scott, W. G. (2010) Small self-cleaving ribozymes, *Cold Spring Harbor Perspectives in Biology*.

(30) Lai, M. M. (1995) The molecular biology of hepatitis delta virus. *Annu. Rev. Biochem. 64*, 259–286.

(31) Taylor, J. M. (2006) Structure and replication of hepatitis delta virus RNA, in *Hepatitis Delta Virus* (Handa, H., and Yamaguchi, Y., Eds.) pp 20−37, Landes Bioscience, Georgetown, TX.

(32) Been, M. D. (2006) HDV ribozymes. *Curr. Top. Microbiol. Immunol. 307*, 47–65.

(33) Salehi-Ashtiani, K., Luptak, A., Litovchick, A., and Szostak, J. W. (2006) A genomewide search for ribozymes reveals an HDV-like sequence in the human CPEB3 gene. *Science 313*, 1788–1792.

(34) Chadalavada, D. M., Gratton, E. A., and Bevilacqua, P. C. (2010) The human HDV-like *CPEB3* ribozyme is intrinsically fast-reacting. *Biochemistry 49*, 5321–5330.

(35) Webb, C.-H. T., Riccitelli, N. J., Ruminski, D. J., and Lupták, A. (2009) Widespread occurrence of self-cleaving ribozymes. *Science 326*, 953.

(36) Perrotta, A. T., Shih, I., and Been, M. D. (1999) Imidazole rescue of a cytosine mutation in a self-cleaving ribozyme. *Science 286*, 123–126.

(37) Nakano, S., Chadalavada, D. M., and Bevilacqua, P. C. (2000) General acid-base catalysis in the mechanism of a hepatitis delta virus ribozyme. *Science 287*, 1493–1497.

(38) Nakano, S., Proctor, D. J., and Bevilacqua, P. C. (2001) Mechanistic characterization of the HDV genomic ribozyme: assessing the catalytic and structural contributions of divalent metal ions within a multichannel reaction mechanism. *Biochemistry 40*, 12022–12038.

(39) Das, S. R., and Piccirilli, J. A. (2005) General acid catalysis by the hepatitis delta virus ribozyme. *Nat. Chem. Biol. 1*, 45–52.

(40) Koo, S., Novak, T., and Piccirilli, J. A. (2008) Catalytic mechanism of the HDV ribozyme, in *Ribozymes and RNA Catalysis* (Lilley, D. M., and Eckstein, F., Eds.) pp 92−122, RSC Publishing, Cambridge, U.K.

(41) Cerrone-Szakal, A. L., Siegfried, N. A., and Bevilacqua, P. C. (2008) Mechanistic characterization of the HDV genomic ribozyme: solvent isotope effects and proton inventories in the absence of divalent metal ions support C75 as the general acid. *J. Am. Chem. Soc. 130*, 14504–14520.

(42) Chen, J. H., Yajima, R., Chadalavada, D. M., Chase, E., Bevilacqua, P. C., and Golden, B. L. (2010) A 1.9 Å crystal structure of the HDV ribozyme pre-cleavage suggests both Lewis acid and general acid mechanisms contribute to phosphodiester bond cleavage. *Biochemistry 49*, 6508–6518.

(43) Luptak, A., Ferre-D'Amare, A. R., Zhou, K., Zilm, K. W., and Doudna, J. A. (2001) Direct pK(a) measurement of the active-site cytosine in a genomic hepatitis delta virus ribozyme. *J. Am. Chem. Soc. 123*, 8447–8452.

(44) Gong, B., Chen, J. H., Chase, E., Chadalavada, D. M., Yajima, R., Golden, B. L., Bevilacqua, P. C., and Carey, P. R. (2007) Direct measurement of a pK(a) near neutrality for the catalytic cytosine in the genomic HDV ribozyme using Raman crystallography. *J. Am. Chem. Soc. 129*, 13335–13342.

(45) Nakano, S., and Bevilacqua, P. C. (2007) Mechanistic characterization of the HDV genomic ribozyme: a mutant of the C41 motif provides insight into the positioning and thermodynamic linkage of metal ions and protons. *Biochemistry 46*, 3001–3012.

(46) Shih, I. H., and Been, M. D. (2001) Involvement of a cytosine side chain in proton transfer in the rate-determining step of ribozyme self-cleavage. *Proc. Natl. Acad. Sci. U.S.A. 98*, 1489–1494.

(47) Nakano, S., and Bevilacqua, P. C. (2001) Proton inventory of the genomic HDV ribozyme in Mg^{2+}-containing solutions. *J. Am. Chem. Soc. 123*, 11333–11334.

(48) Bevilacqua, P. C. (2003) Mechanistic considerations for general acid-base catalysis by RNA: revisiting the mechanism of the hairpin ribozyme. *Biochemistry 42*, 2259–2265.

(49) Suh, Y. A., Kumar, P. K., Taira, K., and Nishikawa, S. (1993) Self-cleavage activity of the genomic HDV ribozyme in the presence of various divalent metal ions. *Nucleic Acids Res. 21*, 3277–3280.

(50) Nakano, S., Cerrone, A. L., and Bevilacqua, P. C. (2003) Mechanistic characterization of the HDV genomic ribozyme: classifying the catalytic and structural metal ion sites within a multichannel reaction mechanism. *Biochemistry 42*, 2982–2994.

(51) Perrotta, A. T., and Been, M. D. (2006) HDV ribozyme activity in monovalent cations. *Biochemistry 45*, 11357–11365.

(52) Cate, J. H., and Doudna, J. A. (1996) Metal-binding sites in the major groove of a large ribozyme domain. *Structure 4*, 1221–1229.

(53) Kieft, J. S., and Tinoco, I., Jr. (1997) Solution structure of a metal-binding site in the major groove of RNA complexed with cobalt-(III) hexammine. *Structure 5*, 713–721.

(54) Keel, A. Y., Rambo, R. P., Batey, R. T., and Kieft, J. S. (2007) A general strategy to solve the phase problem in RNA crystallography. *Structure 15*, 761–772.

(55) Ferre-D'Amare, A. R., Zhou, K., and Doudna, J. A. (1998) Crystal structure of a hepatitis delta virus ribozyme. *Nature 395*, 567–574.

(56) Ferre-D'Amare, A. R., and Doudna, J. A. (2000) Crystallization and structure determination of a hepatitis delta virus ribozyme: use of the RNA-binding protein U1A as a crystallization module. *J. Mol. Biol. 295*, 541–556.

(57) Jorgensen, W. L., Chandrasekhar, J., Madura, J. D., Impey, R. W., and Klein, M. L. (1983) Comparison of simple potential functions for simulating liquid water. *J. Chem. Phys. 79*, 926–935.

(58) Krasovska, M. V., Sefcikova, J., Reblova, K., Schneider, B., Walter, N. G., and Sponer, J. (2006) Cations and hydration in catalytic RNA: molecular dynamics of the hepatitis delta virus ribozyme. *Biophys. J. 91*, 626–638.

(59) Bowers, K. J., Chow, E., Xu, H., Dror, R. O., Eastwood, M. P., Gregersen, B. A., Klepeis, J. L., Kolossvary, I. K., Moraes, M. A., Sacerdoti, F. D., Salmon, J. K., Shan, Y., and Shaw, D. E. (2006) Scalable algorithms for molecular dynamics simulations on commodity clusters, in Proceedings of the ACM/IEEE Conference on Supercomputing (SC06).

(60) (2008) Desmond Molecular Dynamics System, D. E. Shaw Research, New York.

(61) Cornell, W. D., Cieplak, P., Bayly, C. I., Gould, I. R., Merz, K. M. J., Ferguson, D. M., Spellmeyer, D. C., Fox, T., Caldwell, J. W., and Kollman, P. A. (1995) A second generation force field for the simulation of proteins, nucleic acids, and organic molecules. *J. Am. Chem. Soc. 117*, 5179–5197.

(62) Wang, J. M., Cieplak, P., and Kollman, P. A. (2000) How well does a restrained electrostatic potential (RESP) model perform in calculating conformational energies of organic and biological molecules? *J. Comput. Chem. 21*, 1049–1074.

(63) Veeraraghavan, N., Bevilacqua, P. C., and Hammes-Schiffer, S. (2010) Long distance communication in the HDV ribozyme: insights from molecular dynamics and experiments. *J. Mol. Biol. 402*, 278–291.

(64) Bayly, C. I., Cieplak, P., Cornell, W. D., and Kollman, P. A. (1993) A well-behaved electrostatic potential based method using charge restraints for determining atom-centered charges: the RESP model. *J. Phys. Chem. 97*, 10269–10280.

(65) Cieplak, P., Cornell, W. D., Bayly, C., and Kollman, P. A. (1995) Application of the multimolecule and multiconformational RESP methodology to biopolymers: charge derivation for DNA, RNA, and proteins. *J. Comput. Chem. 16*, 1357–1377.

(66) Pigache, A., Cieplak, P., and Dupradeau, F.-Y. (2004) 227th National Meeting of the American Chemical Society, Anaheim, CA.

(67) Darden, T., York, D., and Pedersen, L. (1993) Particle mesh Ewald: an N log (N) method for Ewald sums in large systems. *J. Chem. Phys. 98*, 10089–10092.

(68) Ryckaert, J. P., Ciccotti, G., and Berendsen, H. J. C. (1977) Numerical integration of the Cartesian equations of motion of a system

with constraints: molecular dynamics of n-alkanes. *J. Comput. Phys 23*, 327–341.

(69) Nosé, S. (1984) A molecular dynamics method for simulations in the canonical ensemble. *Mol. Phys. 52*, 255–268.

(70) Hoover, W. G. (1985) Canonical dynamics: equilibrium phase-space distributions. *Phys. Rev. A 31*, 1695–1697.

(71) Chin, K., Sharp, K. A., Honig, B., and Pyle, A. M. (1999) Calculating the electrostatic properties of RNA provides new insights into molecular interactions and function. *Nat. Struct. Biol. 6*, 1055–1061.

(72) Misra, V. K., and Draper, D. E. (2000) Mg(2+) binding to tRNA revisited: the nonlinear Poisson-Boltzmann model. *J. Mol. Biol. 299*, 813–825.

(73) Maderia, M., Hunsicker, L. M., and DeRose, V. J. (2000) Metal-phosphate interactions in the hammerhead ribozyme observed by ^{31}P NMR and phosphorothioate substitutions. *Biochemistry 39*, 12113–12120.

(74) Baker, N. A., Sept, D., Joseph, S., Holst, M. J., and McCammon, J. A. (2001) Electrostatics of nanosystems: application to microtubules and the ribosome. *Proc. Natl. Acad. Sci. U.S.A. 98*, 10037–10041.

(75) Wadkins, T. S., Shih, I., Perrotta, A. T., and Been, M. D. (2001) A pH-sensitive RNA tertiary interaction affects self-cleavage activity of the HDV ribozymes in the absence of added divalent metal ion. *J. Mol. Biol. 305*, 1045–1055.

(76) Alberts, B., Bray, D., Lewis, J., Raff, M., Roberts, K., and Watson, J. D. (1994) in *Molecular Biology of the Cell*, p 508, Garland Publishing, New York.

(77) Feig, A. L., and Uhlenbeck, O. (1999) The role of metal ions in RNA biochemistry, in *The RNA World* (Gesteland, R. F., Cech, T. R., and Atkins, J. F., Eds.) 2nd ed., pp 287−319, Cold Spring Harbor Laboratory Press, Cold Spring Harbor, NY.

(78) Gilson, M. K., Sharp, K. A., and Honig, B. (1987) Calculating the electrostatic potential of molecules in solution: method and error assessment. *J. Comput. Chem. 9*, 327–335.

(79) Gilson, M. K., and Honig, B. (1988) Calculation of the total electrostatic energy of a macromolecular system: solvation energies, binding energies, and conformational analysis. *Proteins 4*, 7–18.

(80) DeLano, W. L. (2002) DeLano Scientific, San Carlos, CA.

(81) Adams, P. D., Afonine, P. V., Bunkoczi, G., Chen, V. B., Davis, I. W., Echols, N., Headd, J. J., Hung, L. W., Kapral, G. J., Grosse-Kunstleve, R. W., McCoy, A. J., Moriarty, N. W., Oeffner, R., Read, R. J., Richardson, D. C., Richardson, J. S., Terwilliger, T. C., and Zwart, P. H. (2010) PHENIX: a comprehensive Python-based system for macromolecular structure solution. *Acta Crystallogr., Sect. D: Biol. Crystallogr. 66*, 213–221.

(82) Otwinowski, Z., and Minor, W. (1997) Processing of X-ray diffraction data collected in oscillation mode, in *Methods in Enzymology, Macromolecular Crystallography* (Carter, C. W. J., and Sweet, R. M., Eds.) Part A, pp 307−326, Academic Press, New York.

(83) Brunger, A. T., Adams, P. D., Clore, G. M., DeLano, W. L., Gros, P., Grosse-Kunstleve, R. W., Jiang, J. S., Kuszewski, J., Nilges, M., Pannu, N. S., Read, R. J., Rice, L. M., Simonson, T., and Warren, G. L. (1998) Crystallography & NMR system: a new software suite for macromolecular structure determination. *Acta Crystallogr., Sect. D: Biol. Crystallogr. 54*, 905–921.

(84) Brunger, A. T. (2007) Version 1.2 of the crystallography and NMR system. *Nat. Protoc. 2*, 2728–2733.

(85) Tanner, N. K., Schaff, S., Thill, G., Petit-Koskas, E., Crain-Denoyelle, A. M., and Westhof, E. (1994) A three-dimensional model of hepatitis delta virus ribozyme based on biochemical and mutational analyses. *Curr. Biol. 4*, 488–498.

(86) Ke, A., Zhou, K., Ding, F., Cate, J. H., and Doudna, J. A. (2004) A conformational switch controls hepatitis delta virus ribozyme catalysis. *Nature 429*, 201–205.

(87) Ke, A., Ding, F., Batchelor, J. D., and Doudna, J. A. (2007) Structural roles of monovalent cations in the HDV ribozyme. *Structure 15*, 281–287.

(88) Krasovska, M. V., Sefcikova, J., Spackova, N., Sponer, J., and Walter, N. G. (2005) Structural dynamics of precursor and product of the RNA enzyme from the hepatitis delta virus as revealed by molecular dynamics simulations. *J. Mol. Biol. 351*, 731–748.

(89) Banas, P., Rulisek, L., Hanosova, V., Svozil, D., Walter, N. G., Sponer, J., and Otyepka, M. (2008) General base catalysis for cleavage by the active-site cytosine of the hepatitis delta virus ribozyme: QM/MM calculations establish chemical feasibility. *J. Phys. Chem. B 112*, 11177–11187.

(90) Brown, T. S., Chadalavada, D. M., and Bevilacqua, P. C. (2004) Design of a highly reactive HDV ribozyme sequence uncovers facilitation of RNA folding by alternative pairings and physiological ionic strength. *J. Mol. Biol. 341*, 695–712.

(91) Megyes, T., Bálint, S., Grósz, T., Randnai, T., and Bakó, I. (2008) The structure of aqueous sodium hydroxide solutions: a combined solution x-ray diffraction and simulation study. *J. Chem. Phys. 128*, 044501.

(92) Adams, P. L., Stahley, M. R., Kosek, A. B., Wang, J., and Strobel, S. A. (2004) Crystal structure of a self-splicing group I intron with both exons. *Nature 430*, 45–50.

(93) Guo, F., Gooding, A. R., and Cech, T. R. (2004) Structure of the *Tetrahymena* ribozyme: base triple sandwich and metal ion at the active site. *Mol. Cell 16*, 351–362.

(94) Reiter, N. J., Osterman, A., Torres-Larios, A., Swinger, K. K., Pan, T., and Mondragon, A. (2010) Structure of a bacterial ribonuclease P holoenzyme in complex with tRNA. *Nature 468*, 784–789.

(95) Murray, J. B., Seyhan, A. A., Walter, N. G., Burke, J. M., and Scott, W. G. (1998) The hammerhead, hairpin and VS ribozymes are catalytically proficient in monovalent cations alone. *Chem. Biol. 5*, 587–595.

(96) Colmenarejo, G., and Tinoco, I., Jr. (1999) Structure and thermodynamics of metal binding in the P5 helix of a group I intron ribozyme. *J. Mol. Biol. 290*, 119–135.

(97) Montange, R. K., and Batey, R. T. (2006) Structure of the S-adenosylmethionine riboswitch regulatory mRNA element. *Nature 441*, 1172–1175.

(98) Stefan, L. R., Zhang, R., Levitan, A. G., Hendrix, D. K., Brenner, S. E., and Holbrook, S. R. (2006) MeRNA: a database of metal ion binding sites in RNA structures. *Nucleic Acids Res. 34*, D131–D134.

(99) Cate, J. H., Gooding, A. R., Podell, E., Zhou, K., Golden, B. L., Kundrot, C. E., Cech, T. R., and Doudna, J. A. (1996) Crystal structure of a group I ribozyme domain: principles of RNA packing. *Science 273*, 1678–1685.

(100) Hougland, J. L., Piccirilli, J. A., Forconi, M., Lee, J., and Herschlag, D. (2006) How the group I intron works: a case study of RNA structure and function, in *RNA World* (Gesteland, R. F., Cech, T. R., and Atkins, J. F., Eds.) 3rd ed., pp 133−205, Cold Spring Harbor Press, Cold Spring Harbor, NY.

(101) Gong, B., Chen, J. H., Bevilacqua, P. C., Golden, B. L., and Carey, P. R. (2009) Competition between Co(NH(3))(6)(3+) and inner sphere Mg(2+) ions in the HDV ribozyme. *Biochemistry 48*, 11961–11970.

(102) Curtis, E. A., and Bartel, D. P. (2001) The hammerhead cleavage reaction in monovalent cations. *RNA 7*, 546–552.

(103) O'Rear, J. L., Wang, S., Feig, A. L., Beigelman, L., Uhlenbeck, O. C., and Herschlag, D. (2001) Comparison of the hammerhead cleavage reactions stimulated by monovalent and divalent cations. *RNA 7*, 537–545.

(104) Tang, C. L., Alexov, E., Pyle, A. M., and Honig, B. (2007) Calculation of pK(a)s in RNA: on the structural origins and functional roles of protonated nucleotides. *J. Mol. Biol. 366*, 1475–1496.